PHOTONICS Research

Quantifying quantum coherence of optical cat states

Miao Zhang,[1,†] **Haijun Kang,**[1,†] **Meihong Wang,**[1,2] **Fengyi Xu,**[1] **Xiaolong Su,**[1,2,*] **and Kunchi Peng**[1,2]

[1]*State Key Laboratory of Quantum Optics and Quantum Optics Devices, Institute of Opto-Electronics, Shanxi University, Taiyuan 030006, China*
[2]*Collaborative Innovation Center of Extreme Optics, Shanxi University, Taiyuan 030006, China*
*Corresponding author: suxl@sxu.edu.cn

The optical cat state plays an essential role in quantum computation and quantum metrology. Here, we experimentally quantify quantum coherence of an optical cat state by means of relative entropy and the l_1 norm of coherence in a Fock basis based on the prepared optical cat state at the rubidium D1 line. By transmitting the optical cat state through a lossy channel, we also demonstrate the robustness of quantum coherence of the optical cat state in the presence of loss, which is different from the decoherence properties of fidelity and Wigner function negativity of the optical cat state. Our results confirm that quantum coherence of optical cat states is robust against loss and pave the way for the application of optical cat states.   © 2021 Chinese Laser Press

1. INTRODUCTION

As a superposition of two coherent states, the optical cat state is an important quantum resource for quantum information processing, including quantum computation [1–3], quantum teleportation [4–6], and quantum metrology [7]. An optical cat state can be experimentally prepared by photon subtraction from a squeezed vacuum state [8–13]. It has been shown that the amplitude of optical cat states can be increased by time-separated two-photon subtraction [14] and three-photon subtraction [15]. Meanwhile, optical squeezed cat states are generated by different means [16–18]. Based on the prepared optical cat states, several applications have been experimentally demonstrated, including quantum teleportation of cat states [19], tele-amplification [20], preparation of hybrid entangled states and teleportation based on it [21–24], amplification of cat states [25], and the Hadamard gate [26].

Quantum coherence, which encapsulates the idea of super-position of quantum states, is a defining feature of quantum mechanics and plays a key role in applications of quantum physics and quantum information [27]. The resource theory of quantum coherence has attracted considerable interest recently [28–36]. The relations between quantum coherence and other quantum resources are extensively discussed, such as entanglement [32,33], asymmetry [34,35], and path information [36]. Several experiments related to quantum coherence have been demonstrated, including obtainment of maximal coherence via an assisted distillation process [37], observability and operability of robustness of coherence [38], wave-particle

duality relation based on coherence measurement [39], the trade-off relation for quantum coherence [40], the relation between coherence and path information [41], the resilience effect of quantum coherence to transversal noise [42], the relation between quantum non-Markovianity and coherence [43], experimental control of the degree of non-classicality via quantum coherence [44], estimation of quantum coherence by collective measurements [45], and quantification of coherence of a tunable quantum detector [46]. The roles of quantum coherence in the Deutsch–Jozsa algorithm [47] and Grover quantum search algorithm [48] have also been discussed recently.

For application, it is crucial to quantify quantum coherence of various quantum states expressed in finite and infinite dimensional systems [28–31]. Very recently, Tan *et al.* proposed an approach to quantify the coherence between coherent states based on the Glauber–Sudarshan P distribution [49], which can be used to quantify quantum coherence of the cat state. For the preparation of a cat state, the density matrix in a Fock basis can be obtained directly in the process of quantum tomography. Thus, it is convenient to quantify quantum coherence of cat states in a Fock basis. At the same time, it has been shown that the Wigner function negativity of the optical cat state is sensitive to loss [50,51]. However, the effect of loss on the quantum coherence of optical cat states is unclear. As a consequence, it is essential to investigate the evolution of quantum coherence of cat states in the presence of loss.

In this paper, we prepare an optical cat state at the rubidium D1 line, which is a crucial medium for quantum memory. Then we experimentally demonstrate quantification of

quantum coherence of the optical cat state in a Fock basis by relative entropy and the l_1 norm calculated from the density matrix. Finally, the evolution of quantum coherence of the optical cat state in a lossy channel is investigated. By transmitting the prepared optical cat state with amplitude of 1.06 and fidelity of 0.68 through a lossy channel, we show that quantum coherence of the cat state is robust against loss. Comparing with the fidelity and Wigner function negativity of the cat state in a lossy channel, we show that when the fidelity is below 0.5 and the negativity disappears, the quantum coherence of the cat state still exists. The presented results provide a useful reference for the application of the optical cat state.

2. PRINCIPLE AND EXPERIMENTAL SETUP

The relative entropy of quantum coherence refers to the distance between quantum states $\hat{\rho}$ and $\hat{\rho}_{\text{diag}}$ formed from the diagonal elements of $\hat{\rho}$ [28], which is given by

$$C_{\text{rel.ent.}}(\hat{\rho}) = S(\hat{\rho}_{\text{diag}}) - S(\hat{\rho}), \qquad (1)$$

where S is the von Neumann entropy, defined by $S(\hat{\rho}) = -\text{Tr}(\hat{\rho}\log_2\hat{\rho})$.

The l_1 norm of quantum coherence depends on the magnitudes of off-diagonal density matrix elements [28], given by

$$C_{l_1}(\hat{\rho}) = \sum_{\substack{m,n \\ m\neq n}} |\rho_{m,n}|. \qquad (2)$$

For a cat state, generally, it is represented in an infinite dimensional Fock basis. But in experiment, the obtained density matrix of the cat state is truncated in a finite dimension by performing quantum state tomography. Thus, the relative entropy and l_1 norm in a Fock basis can be applied to quantify the quantum coherence of cat states.

A schematic of the decoherence process of an optical odd cat state in a lossy channel is shown in Fig. 1(a). An ideal odd cat state has an obvious Wigner function negativity and quantum interference between two coherent states. When it is transmitted through a lossy channel with 50% transmission efficiency, the Wigner function negativity and quantum interference disappear, and the distance of two coherent states is shortened.

When an ideal cat state with amplitude of α is transmitted through a lossy channel with a transmission efficiency of η, its density matrix can be expressed as [52]

$$\hat{\rho}(\alpha,\eta) = (1 - P_{\pm})\hat{\rho}_{\pm}\left(\sqrt{\eta}\alpha\right) + P_{\pm}\hat{\rho}_{\mp}\left(\sqrt{\eta}\alpha\right), \qquad (3)$$

where $P_{\pm} = \frac{N_{\mp}(\sqrt{\eta}\alpha)}{2N_{\pm}(\alpha)}[1 - e^{-2(1-\eta)\alpha^2}]$ is a probability of the initial even (odd) cat state converted to an odd (even) cat state, $\hat{\rho}_{\pm}(\sqrt{\eta}\alpha) = \frac{1}{N_{\pm}(\sqrt{\eta}\alpha)}(|\sqrt{\eta}\alpha\rangle \pm |-\sqrt{\eta}\alpha\rangle)(\langle\sqrt{\eta}\alpha| \pm \langle-\sqrt{\eta}\alpha|)$ is the density matrix of an even (odd) cat state with an amplitude of $\sqrt{\eta}\alpha$, and $N_{\pm}(\alpha) = 2(1 \pm e^{-2\alpha^2})$ is the normalization factor. According to the density matrix, we can directly calculate the quantum coherence of the cat state in a lossy channel based on relative entropy and the l_1 norm. The relative entropy and l_1 norm of quantum coherence for the odd cat state are given by

$$C_{\text{rel.ent.}}(\alpha,\eta) = (1 - P_-)C^{\text{odd}}_{\text{rel.ent.}}(\sqrt{\eta}\alpha) + P_-C^{\text{even}}_{\text{rel.ent.}}(\sqrt{\eta}\alpha), \qquad (4)$$
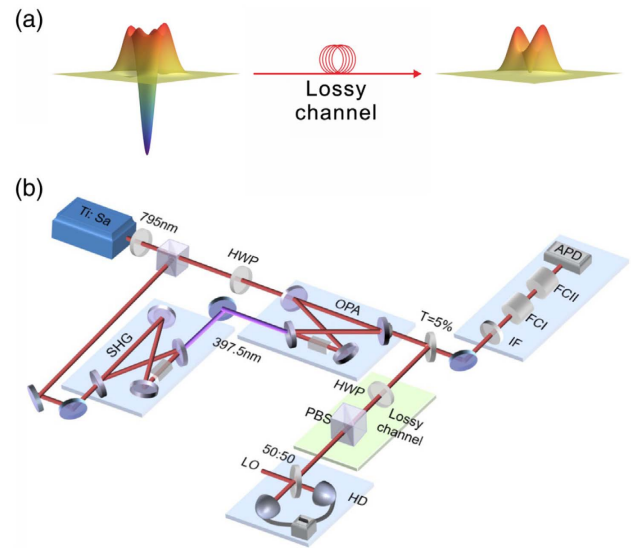
Fig. 1. (a) Illustration of the decoherence process of optical cat state in phase space. An ideal optical odd cat state with amplitude $\alpha = 1$ transmits through a lossy channel with transmission efficiency of 50%, and the Wigner functions are displayed before and after transmission. (b) Experimental setup. A lossy channel consists of a half-wave plate (HWP) and a polarization beam splitter (PBS). OPA, optical parameter amplification with cavity length of 480 mm; SHG, second harmonic generator with cavity length of 480 mm; IF, interference filter (0.4 nm); FC, filter cavity with cavity length of 0.75 mm; FC2, filter cavity with cavity length of 2.05 mm; HD, homodyne detector; LO, local oscillator; APD, avalanche photodiode.

$$C_{l_1}(\alpha,\eta) = (1 - P_-)C^{\text{odd}}_{l_1}(\sqrt{\eta}\alpha) + P_-C^{\text{even}}_{l_1}(\sqrt{\eta}\alpha), \qquad (5)$$

respectively. The $C^{\text{odd}}_{\text{rel.ent.}}(\sqrt{\eta}\alpha)$ and $C^{\text{even}}_{\text{rel.ent.}}(\sqrt{\eta}\alpha)$ are the relative entropy of coherence of the odd cat state and the even cat state with amplitude of $\sqrt{\eta}\alpha$, respectively. The $C^{\text{odd}}_{l_1}(\sqrt{\eta}\alpha)$ and $C^{\text{even}}_{l_1}(\sqrt{\eta}\alpha)$ are the l_1 norm of coherence of the odd cat state and even cat state with amplitude of $\sqrt{\eta}\alpha$, respectively. The expressions of quantum coherence of the odd and even cat states can be found in Appendix B.

Usually, the fidelity and Wigner function negativity are used to characterize a cat state. The fidelity of the odd cat state refers to the overlap between the quantum state $\hat{\rho}$ and an ideal odd cat state $\hat{\rho}_-$ and can be defined as $F = \text{Tr}[\hat{\rho}\hat{\rho}_-]$. The fidelity of the odd cat state in a lossy channel is given by

$$F = \cosh[-\alpha^2(1 - \eta)]\frac{\sinh\eta\alpha^2}{\sinh\alpha^2}, \qquad (6)$$

which is obtained by calculating the overlap between the output state transmitting through the lossy channel and an ideal odd cat state $\hat{\rho}_-(\sqrt{\eta}\alpha)$. The negativity of the Wigner function shows the nonclassical character of a quantum state [53]. It is denoted as the minimum of Wigner function $W(x,p)$, where x and p are the position and momentum parameters in phase space, respectively. The negativity of the odd cat state in a lossy channel is denoted as

$$W_N = \min\{0, W(0,0)\}, \qquad (7)$$

where $W(0,0) = \frac{1}{\pi N_-}e^{-2\alpha^2\eta}[2 - 2e^{-2\alpha^2(1-2\eta)}]$.

The schematic of our experimental setup is shown in Fig. 1(b). A continuous wave single frequency Ti:sapphire laser operated at 795 nm corresponding to the rubidium D1 line is used as the light source. A squeezed vacuum state with –3 dB squeezing is generated by a frequency-degenerate optical parameter amplifier (OPA) that contains a periodically poled KTiOPO$_4$ (PPKTP) crystal with a pump power of 25 mW. By subtracting a photon from the squeezed state through a beam splitter with a transmissivity of 5%, an optical cat state is experimentally prepared, which is measured by a homodyne detector when a photon is detected by an avalanche photodiode (APD) in the trigger path. The generation rate of the cat state is around 2 kHz (the maximum dark count is 60 Hz). We take 50,000 photocurrents to obtain the density matrix in a Fock basis with a photon number cutoff of 11 using the iterative maximum-likelihood algorithm [54] corrected for 80% detection efficiency. The Wigner function of the cat state is reconstructed from the density matrix. More details of the experimental parameters can be found in Appendix A.
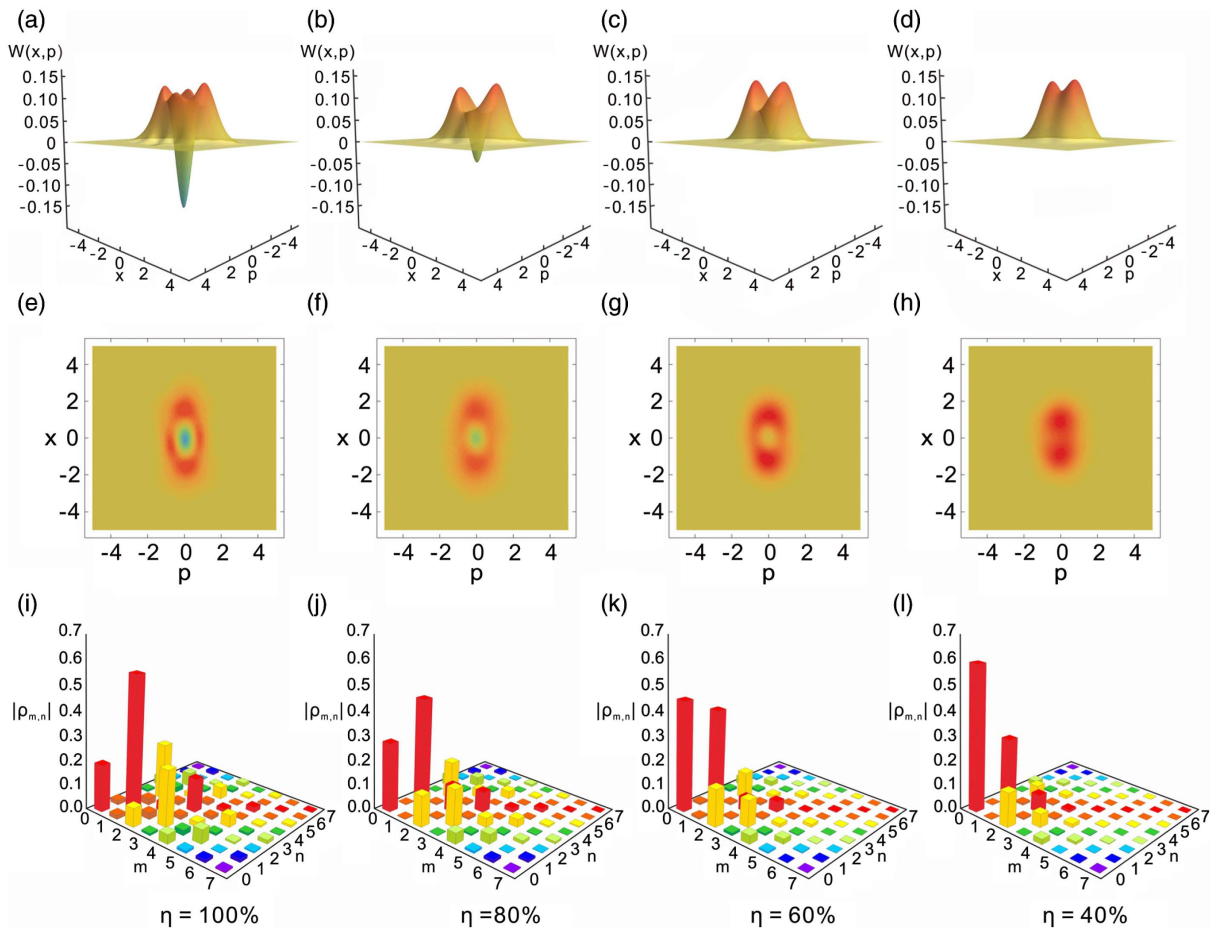
3. RESULTS

An optical cat state with amplitude of 1.06 ± 0.01 and fidelity of 0.68 ± 0.01 is prepared in our experiment; the corresponding Wigner function, projection of the Wigner function, and absolute values of the density matrix elements in the Fock basis are shown in Figs. 2(a), 2(e), and 2(i), respectively. In Fig. 2(a), we can see the obvious quantum interference between two coherent states and a negative value of the Wigner function, which is –0.16.

The decoherence of the prepared cat state transmitting through a lossy channel with transmission efficiencies of 80%, 60%, and 40% is shown in Fig. 2. We can find the Wigner functions are clearly varied with the loss. The Wigner functions' negativity decreases with the decrease in transmission efficiency, and it disappears when the transmission efficiencies are 60% and 40%. The phase space distance between the two coherent states ($|\alpha\rangle$ and $|-\alpha\rangle$) becomes smaller with the decrease in transmission efficiency. In Figs. 2(i)–2(l), it is obvious that the probability of Fock state $|1\rangle\langle 1|$ decreases and the probability of vacuum state $|0\rangle\langle 0|$ increases with the decrease in transmission efficiency.

Quantum coherence of the prepared cat state is quantified by relative entropy and the l_1 norm according to Eqs. (1) and (2), which are 0.63 and 1.67, respectively. The dependence of quantum coherence (including relative entropy and the l_1 norm), fidelity, and negativity of the Wigner function of the output states on transmission efficiency for the prepared cat state (red solid curve) and an ideal cat state (black dashed curve)

Fig. 2. Experimental results. (a)–(d) Wigner functions $W(x, p)$, (e)–(h) projections, and (i)–(l) absolute values of the density matrix elements in the Fock basis when the transmission efficiencies are 100%, 80%, 60%, and 40%, respectively. All the results are corrected for 80% detection efficiency. Only the subspace up to seven photons is shown.
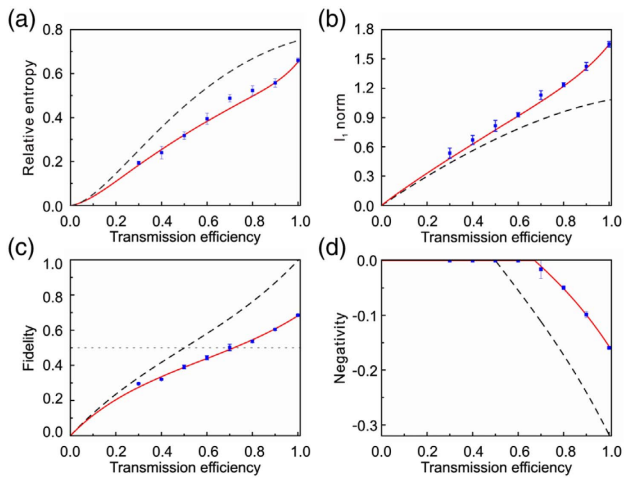
Fig. 3. Dependence of relative entropy, l_1 norm, fidelity, and negativity of cat states on the transmission efficiency. The red solid curve and black dashed curve correspond to the experimentally prepared cat state and the ideal cat state, respectively. The blue dots represent the experimental results.

with amplitude of 1.06 is shown in Figs. 3(a)–3(d), respectively. The relative entropy, l_1 norm, and fidelity of the cat state all decrease with the decrease in transmission efficiency. The negativity tends to zero with the decrease in transmission efficiency. It is interesting that the coherence still exists when the fidelity is lower than 0.5 [corresponding to negativity equal to zero for ideal cat states, dotted line in Fig. 3(c)] and negativity disappears, which confirms the quantum coherence is robust against loss.

As shown in Fig. 3, the theoretical curves of the experimentally prepared cat state and an ideal cat state with the same amplitude are different, which is because of the difference between the prepared cat state and an ideal cat state. The curve of the relative entropy of coherence of the prepared cat state is lower than that of the ideal cat state. However, the curve of the l_1 norm of coherence of the prepared cat state is higher than that of the ideal cat state. This means that the quantification of quantum coherence of an optical cat state is a little bit different using the relative entropy and l_1 norm of coherence. However, the evolution trends of quantum coherence of the optical cat state quantified by these two means are the same in a lossy channel.

4. CONCLUSION

In summary, we experimentally prepare an optical cat state with amplitude of 1.06 and fidelity of 0.68 at the rubidium D1 line. Then we quantify quantum coherence of the cat state by the relative entropy and l_1 norm in the Fock basis. The quantum coherence, fidelity, and Wigner function negativity of the optical cat state in a lossy channel are compared. The experimental results show that quantum coherence of an optical cat state is a robust quantum resource in a lossy environment, since it still exists when the Wigner function negativity of the cat state disappears. We show that the evolution trends of quantum coherence of cat states with relative entropy and the l_1 norm are the

same. Our results are a step closer to applications based on the quantum coherence of cat states.

APPENDIX A: DETAILS OF EXPERIMENT

A solid-state titanium-sapphire continuous wave laser generates a 795 nm light source corresponding to the rubidium D1 line, which is divided into two parts. The first part is injected into a second harmonic generator (SHG) cavity with a cavity length of 480 mm, which contains two concave mirrors ($R = 50$ mm), a high reflectivity mirror, a plane mirror with transmissivity of 8%, and a PPKTP (1 mm × 2 mm × 10 mm) crystal. The second part passes through the model cleaner and is divided into the local oscillator of a homodyne detector and signal beam of a frequency degenerate OPA. The signal beam is periodically chopped by two acousto-optic modulators (AOMs), which defines distinct time bins by the presence and absence of the signal beam, and thus enables the alternate sequence of locking and photon counting without the signal beam. When the signal beam is absent, we generate a nearly pure squeezed vacuum state with –3 dB squeezing by an OPA with a cavity length of 480 mm, which contains two concave mirrors ($R = 50$ mm), a high reflectivity mirror, a plane mirror with transmissivity of 12.5%, and a PPKTP crystal. The OPA works on the parametric amplification status in our experiment, which is guaranteed by locking the relative phase between the pump beam and signal beam to zero.

A beam splitter composed of a half-wave plate and a polarization beam splitter (PBS) transmits 5% of the squeezed vacuum state toward an APD through a filtering system for photon counting. The filter system consists of an interference filter (0.4 nm) and two filter cavities with fineness of 1200, whose cavity lengths are 0.75 mm and 2.05 mm.

The reflected beam by the beam splitter is measured by a homodyne detector when a photon is detected by the APD. The bandwidth of the homodyne detector is 30 MHz and the detection efficiency is about 80%, which includes four parts: interference efficiency between the signal light and local light (98.5%), quantum efficiency of photodiodes (92%, S3883), 19 dB clearance with the 16 mW local oscillator at 13 MHz of the homodyne detector (corresponding to equivalent efficiency 98.7%), and transmission efficiency (91%). Using the maximum likelihood algorithm, we obtain the density matrix and the associated Wigner function.

APPENDIX B: QUANTUM COHERENCE OF CAT STATES

Optical cat states can be expressed as a quantum superposition of two coherent states:

$$|\Psi\rangle = \frac{1}{\sqrt{N\pm}}(|\alpha\rangle \pm |-\alpha\rangle), \tag{B1}$$

where $N_{\pm} = 2(1 \pm e^{-2|\alpha|^2})$ are the normalization factors, and + and – correspond to the even and odd cat states, respectively. Even and odd cat states can be expressed in a Fock basis as [55]

$$|\Psi_+\rangle = \frac{1}{\sqrt{\cosh|\alpha|^2}} \sum_{n=0}^{\infty} \frac{\alpha^n}{\sqrt{n!}} \delta_{0n}^{[2]} |n\rangle, \tag{B2}$$

$$|\Psi_-\rangle = \frac{1}{\sqrt{\sinh|\alpha|^2}} \sum_{n=0}^{\infty} \frac{\alpha^n}{\sqrt{n!}} \delta_{1n}^{[2]}|n\rangle, \tag{B3}$$

respectively. $\delta_{0n}^{[2]} = 0$, $\delta_{1n}^{[2]} = 1$ when n is odd and $\delta_{0n}^{[2]} = 1$, $\delta_{1n}^{[2]} = 0$ when n is even.

Although an ideal cat state is expressed in the infinite dimensional Fock basis, it can be expressed in the finite dimension when the density matrix can characterize the information of the cat state. For example, the odd cat state with amplitude of 1.3 is represented by a density matrix with 11 dimensions [10], and the even cat state with amplitude of 1.61 is represented by a density matrix with 10 dimensions [14]. For an odd cat state with amplitude of α, the density matrix elements are expressed as $\frac{1}{\sinh|\alpha|^2} \frac{\alpha^{m+n}}{\sqrt{m!n!}} \delta_{1m}^{[2]} \delta_{1n}^{[2]}$, and the probability of the $p_{|n\rangle\langle n|}$ is $\frac{1}{\sinh|\alpha|^2} \frac{\alpha^{2n}}{n!} \delta_{1n}^{[2]}$. In the experiment, it is truncated to dimension d (corresponding to a photon-number cutoff of $d-1$) when the probability of higher photons $(d, \ldots, \infty)$ is small enough to be ignored (e.g., 10^{-3}).
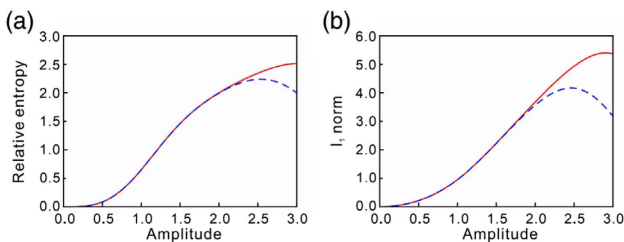
Considering d-dimensional Hilbert space, the relative entropy of coherence of the even and odd cat states can be expressed as

$$C_{\text{rel.ent.}}^{\text{even}}(\alpha) = \frac{1}{\cosh|\alpha|^2}\left(\sum_{n=0}^{d-1} \frac{\alpha^{2n}}{n!} \delta_{0n}^{[2]} \log_2 \cosh|\alpha|^2 \right.$$
$$\left. - \sum_{n=0}^{d-1} \frac{\alpha^{2n}}{n!} \delta_{0n}^{[2]} \log_2 \frac{\alpha^{2n}}{n!}\right), \tag{B4}$$

$$C_{\text{rel.ent.}}^{\text{odd}}(\alpha) = \frac{1}{\sinh|\alpha|^2}\left(\sum_{n=0}^{d-1} \frac{\alpha^{2n}}{n!} \delta_{1n}^{[2]} \log_2 \sinh|\alpha|^2 \right.$$
$$\left. - \sum_{n=0}^{d-1} \frac{\alpha^{2n}}{n!} \delta_{1n}^{[2]} \log_2 \frac{\alpha^{2n}}{n!}\right). \tag{B5}$$

The l_1 norm of coherence of the even and odd cat states can be expressed as

$$C_{l_1}^{\text{even}}(\alpha) = \frac{1}{\cosh|\alpha|^2} \sum_{\substack{m,n=0 \\ m\neq n}}^{d-1} \frac{\alpha^{m+n}}{\sqrt{m!n!}} \delta_{0m}^{[2]} \delta_{0n}^{[2]}, \tag{B6}$$

$$C_{l_1}^{\text{odd}}(\alpha) = \frac{1}{\sinh|\alpha|^2} \sum_{\substack{m,n=0 \\ m\neq n}}^{d-1} \frac{\alpha^{m+n}}{\sqrt{m!n!}} \delta_{1m}^{[2]} \delta_{1n}^{[2]}. \tag{B7}$$

The dependence of relative entropy and the l_1 norm of quantum coherence of an odd cat state on its amplitude with different dimensions is shown in Fig. 4. We can see that when the amplitude is less than two, the quantum coherences of cat states in the 16- or 12-dimensional Hilbert space are the same, which indicates the 12-dimensional Hilbert space we used in our experiment is enough to estimate the quantum coherence of cat states with small amplitudes.

Disclosures. The authors declare no conflicts of interest.

†These authors contributed equally to this work.

REFERENCES

1. T. C. Ralph, A. Gilchrist, G. J. Milburn, W. J. Munro, and S. Glancy, "Quantum computation with optical coherent states," Phys. Rev. A **68**, 042319 (2003).
2. H. Jeong and M. S. Kim, "Efficient quantum computation using coherent states," Phys. Rev. A **65**, 042305 (2002).
3. A. P. Lund, T. C. Ralph, and H. L. Haselgrove, "Fault-tolerant linear optical quantum computing with small-amplitude coherent states," Phys. Rev. Lett. **100**, 030503 (2008).
4. S. L. Braunstein and H. J. Kimble, "Teleportation of continuous quantum variables," Phys. Rev. Lett. **80**, 869–872 (1998).
5. S. J. van Enk and O. Hirota, "Entangled coherent states: teleportation and decoherence," Phys. Rev. A **64**, 022313 (2001).
6. P. van Loock, N. Lütkenhaus, W. J. Munro, and K. Nemoto, "Quantum repeaters using coherent-state communication," Phys. Rev. A **78**, 062319 (2008).
7. A. Gilchrist, K. Nemoto, W. J. Munro, T. C. Ralph, S. Glancy, S. L. Braunstein, and G. J. Milburn, "Schrödinger cats and their power for quantum information processing," J. Opt. B **6**, S828–S833 (2004).
8. M. Dakna, T. Anhut, T. Opatrný, L. Knöll, and D.-G. Welsch, "Generating Schrödinger-cat-like states by means of conditional measurements on a beam splitter," Phys. Rev. A **55**, 3184–3194 (1997).
9. A. Ourjoumtsev, R. Tualle-Brouri, J. Laurat, and P. Grangier, "Generating optical Schrödinger kittens for quantum information processing," Science **312**, 83–86 (2006).
10. J. S. Neergaard-Nielsen, B. M. Nielsen, C. Hettich, K. Mølmer, and E. S. Polzik, "Generation of a superposition of odd photon number states for quantum information networks," Phys. Rev. Lett. **97**, 083604 (2006).
11. K. Wakui, H. Takahashi, A. Furusawa, and M. Sasaki, "Photon subtracted squeezed states generated with periodically poled KTiOPO₄," Opt. Express **15**, 3568–3574 (2007).
12. W. Asavanant, K. Nakashima, Y. Shiozawa, J.-I. Yoshikawa, and A. Furusawa, "Generation of highly pure Schrödinger's cat states and real-time quadrature measurements via optical filtering," Opt. Express **25**, 32227–32242 (2017).
13. T. Serikawa, J.-I. Yoshikawa, S. Takeda, H. Yonezawa, T. C. Ralph, E. H. Huntington, and A. Furusawa, "Generation of a cat state in an optical sideband," Phys. Rev. Lett. **121**, 143602 (2018).
14. H. Takahashi, K. Wakui, S. Suzuki, M. Takeoka, K. Hayasaka, A. Furusawa, and M. Sasaki, "Generation of large-amplitude coherent-state superposition via ancilla-assisted photon subtraction," Phys. Rev. Lett. **101**, 233605 (2008).

Fig. 4. Dependence of relative entropy and l_1 norm of quantum coherence of an optical cat state on its amplitude. The red solid and blue dashed curves correspond the results in the 16-dimensional and 12-dimensional Hilbert space, respectively.

15. T. Gerrits, S. Glancy, T. S. Clement, B. Calkins, A. E. Lita, A. J. Miller, A. L. Migdall, S. W. Nam, R. P. Mirin, and E. Knill, "Generation of optical coherent-state superpositions by number-resolved photon subtraction from the squeezed vacuum," Phys. Rev. A **82**, 031802 (2010).

16. A. Ourjoumtsev, H. Jeong, R. Tualle-Brouri, and P. Grangier, "Generation of optical 'Schrödinger cats' from photon number states," Nature **448**, 784–786 (2007).

17. J. Etesse, M. Bouillard, B. Kanseri, and R. Tualle-Brouri, "Experimental generation of squeezed cat states with an operation allowing iterative growth," Phys. Rev. Lett. **114**, 193602 (2015).

18. K. Huang, H. Le Jeannic, J. Ruaudel, V. B. Verma, M. D. Shaw, F. Marsili, S. W. Nam, E. Wu, H. Zeng, Y.-C. Jeong, R. Filip, O. Morin, and J. Laurat, "Optical synthesis of large-amplitude squeezed coherent-state superpositions with minimal resources," Phys. Rev. Lett. **115**, 023602 (2015).

19. N. Lee, H. Benichi, Y. Takeno, S. Takeda, J. Webb, E. Huntington, and A. Furusawa, "Teleportation of nonclassical wave packets of light," Science **332**, 330–333 (2011).

20. J. S. Neergaard-Nielsen, Y. Eto, C.-W. Lee, H. Jeong, and M. Sasaki, "Quantum tele-amplification with a continuous-variable superposition state," Nat. Photonics **7**, 439–443 (2013).

21. H. Jeong, A. Zavatta, M. Kang, S.-W. Lee, L. S. Costanzo, S. Grandi, T. C. Ralph, and M. Bellini, "Generation of hybrid entanglement of light," Nat. Photonics **8**, 564–569 (2014).

22. O. Morin, K. Huang, J. Liu, H. L. Jeannic, C. Fabre, and J. Laurat, "Remote creation of hybrid entanglement between particle-like and wave-like optical qubits," Nat. Photonics **8**, 570–574 (2014).

23. A. E. Ulanov, D. Sychev, A. A. Pushkina, I. A. Fedorov, and A. I. Lvovsky, "Quantum teleportation between discrete and continuous encodings of an optical qubit," Phys. Rev. Lett. **118**, 160501 (2017).

24. D. V. Sychev, A. E. Ulanov, E. S. Tiunov, A. A. Pushkina, A. Kuzhamuratov, V. Novikov, and A. I. Lvovsky, "Entanglement and teleportation between polarization and wave-like encodings of an optical qubit," Nat. Commun. **9**, 3672 (2018).

25. D. V. Sychev, A. E. Ulanov, A. A. Pushkina, M. W. Richards, I. A. Fedorow, and A. I. Lvovsky, "Enlargement of optical Schrödinger's cat states," Nat. Photonics **11**, 379–382 (2017).

26. A. Tipsmark, R. Dong, A. Laghaout, P. Marek, M. Ježek, and U. L. Andersen, "Experimental demonstration of a Hadamard gate for coherent state qubits," Phys. Rev. A **84**, 050301 (2011).

27. A. Streltsov, G. Adesso, and M. B. Plenio, "Colloquium: quantum coherence as a resource," Rev. Mod. Phys. **89**, 041003 (2017).

28. T. Baumgratz, M. Cramer, and M. B. Plenio, "Quantifying coherence," Phys. Rev. Lett. **113**, 140401 (2014).

29. D. Girolami, "Observable measure of quantum coherence in finite dimensional systems," Phys. Rev. Lett. **113**, 170401 (2014).

30. J. Xu, "Quantifying coherence of Gaussian states," Phys. Rev. A **93**, 032111 (2016).

31. Y.-R. Zhang, L.-H. Shao, Y. Li, and H. Fan, "Quantifying coherence in infinite-dimensional systems," Phys. Rev. A **93**, 012334 (2016).

32. A. Streltsov, U. Singh, H. S. Dhar, M. N. Bera, and G. Adesso, "Measuring quantum coherence with entanglement," Phys. Rev. Lett. **115**, 020403 (2015).

33. K. C. Tan and H. Jeong, "Entanglement as the symmetric portion of correlated coherence," Phys. Rev. Lett. **121**, 220401 (2018).

34. K. Bu, N. Anand, and U. Singh, "Asymmetry and coherence weight of quantum states," Phys. Rev. A **97**, 032342 (2018).

35. M. Lostaglio and M. P. Müller, "Coherence and asymmetry cannot be broadcast," Phys. Rev. Lett. **123**, 020403 (2019).

36. E. Bagan, J. A. Bergou, S. S. Cottrell, and M. Hillery, "Relations between coherence and path information," Phys. Rev. Lett. **116**, 160406 (2016).

37. K.-D. Wu, Z. Hou, H.-S. Zhong, Y. Yuan, G.-Y. Xiang, C.-F. Li, and G.-C. Guo, "Experimentally obtaining maximal coherence via assisted distillation process," Optica **4**, 000454 (2017).

38. W. Zheng, Z. Ma, H. Wang, S.-M. Fei, and X. Peng, "Experimental demonstration of observability and operability of robustness of coherence," Phys. Rev. Lett. **120**, 230504 (2018).

39. Y. Yuan, Z. Hou, Y.-Y. Zhao, H.-S. Zhong, G.-Y. Xiang, C.-F. Li, and G.-C. Guo, "Experimental demonstration of wave-particle duality relation based on coherence measure," Opt. Express **26**, 004470 (2018).

40. W.-M. Lv, C. Zhang, X.-M. Hu, H. Cao, J. Wang, Y.-F. Huang, B.-H. Liu, C.-F. Li, and G.-C. Guo, "Experimental test of the trade-off relation for quantum coherence," Phys. Rev. A **98**, 062337 (2018).

41. J. Gao, Z.-Q. Jiao, C.-Q. Hu, L.-F. Qiao, R.-J. Ren, H. Tang, Z.-H. Ma, S.-M. Fei, V. Vedral, and X.-M. Jin, "Experimental test of the relation between coherence and path information," Commun. Phys. **1**, 89 (2018).

42. C. Zhang, T. R. Bromley, Y.-F. Huang, H. Cao, W.-M. Lv, B.-H. Liu, C.-F. Li, G.-C. Guo, M. Cianciaruso, and G. Adesso, "Demonstrating quantum coherence and metrology that is resilient to transversal noise," Phys. Rev. Lett. **123**, 180504 (2019).

43. K.-D. Wu, Z. Hou, G.-Y. Xiang, C.-F. Li, G.-C. Guo, D. Dong, and F. Nori, "Detecting non-Markovianity via quantified coherence: theory and experiments," npj Quantum Inf. **6**, 55 (2020).

44. A. Smirne, T. Nitsche, D. Egloff, S. Barkhofen, S. De, I. Dhand, C. Silberhorn, S. F. Huelga, and M. B. Plenio, "Experimental control of the degree of non-classicality via quantum coherence," Quantum Sci. Technol. **5**, 04LT01 (2020).

45. Y. Yuan, Z. Hou, J.-F. Tang, A. Streltsov, G.-Y. Xiang, C.-F. Li, and G.-C. Guo, "Direct estimation of quantum coherence by collective measurements," npj Quantum Inf. **6**, 46 (2020).

46. H. Xu, F. Xu, T. Theurer, D. Egloff, Z.-W. Liu, N. Yu, M. B. Plenio, and L. Zhang, "Experimental quantification of coherence of a tunable quantum detector," Phys. Rev. Lett. **125**, 060404 (2020).

47. M. Hillery, "Coherence as a resource in decision problems: the Deutsch-Jozsa algorithm and a variation," Phys. Rev. A **93**, 012111 (2016).

48. H.-L. Shi, S.-Y. Liu, X.-H. Wang, W.-L. Yang, Z.-Y. Yang, and H. Fan, "Coherence depletion in the Grover quantum search algorithm," Phys. Rev. A **95**, 032307 (2017).

49. K. C. Tan, T. Volkoff, H. Kwon, and H. Jeong, "Quantifying the coherence between coherent states," Phys. Rev. Lett. **119**, 190405 (2017).

50. H. Le Jeannic, A. Cavaillès, K. Huang, R. Filip, and J. Laurat, "Slowing quantum decoherence by squeezing in phase space," Phys. Rev. Lett. **120**, 073603 (2018).

51. A. Serafini, S. D. Siena, F. Illuminati, and M. G. A. Paris, "Minimum decoherence cat-like states in Gaussian noisy channels," J. Opt. B **6**, S591–S596 (2004).

52. S. Glancy, H. M. Vasconcelos, and T. C. Ralph, "Transmission of optical coherent-state qubits," Phys. Rev. A **70**, 022317 (2004).

53. K. C. Tan, S. Choi, and H. Jeong, "Negativity of quasiprobability distributions as a measure of nonclassicality," Phys. Rev. Lett. **124**, 110404 (2020).

54. A. I. Lvovsky and M. G. Raymer, "Continuous-variable optical quantum-state tomography," Rev. Mod. Phys. **81**, 299–332 (2009).

55. J. S. Neergaard-Nielsen, "Generation of single photons and Schrödinger kitten states of light," Ph.D. thesis (University of Copenhagen, 2008).